DOE/MC/31160--5222

PARTICULATE HOT GAS STREAM CLEANUP TECHNICAL ISSUES

QUARTERLY REPORT

July 1995 - September 1995

SRI-ENV-95-891-8484-Q4

December 15, 1995

SOUTHERN RESEARCH INSTITUTE
2000 NINTH AVENUE SOUTH
Post Office Box 55305
BIRMINGHAM, ALABAMA 35255-5305
Principal Investigator: D. H. Pontius

for

UNITED STATES DEPARTMENT OF ENERGY
Morgantown Energy Technology Center
Post Office Box 880, 3610 Collins Ferry Road
Morgantown, West Virginia 26505

Contract No. DE-AC21-94MC31160
Project Manager: Thomas P. Dorchak

Contract No. DE-AC21-94MC31160

PARTICULATE HOT GAS STREAM CLEANUP TECHNICAL ISSUES

QUARTERLY REPORT

July 1995 - September 1995

Prepared for

UNITED STATES DEPARTMENT OF ENERGY
Morgantown Energy Technology Center
Post Office Box 880, 3610 Collins Ferry Road
Morgantown, West Virginia 26505

PARTICULATE HOT GAS STREAM CLEANUP TECHNICAL ISSUES

QUARTERLY REPORT

July 1995 - September 1995

SRI-ENV-95-891-8484-Q4

Contract No. DE-AC21-94MC31160

December 15, 1995

Approved by

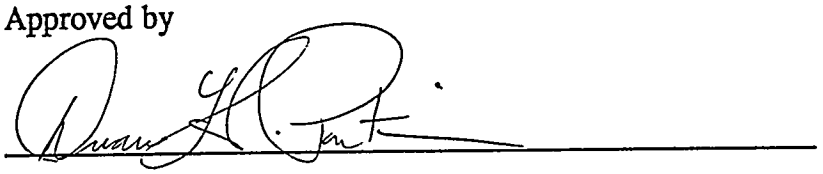

Duane H. Pontius, Director Particulate Sciences Department

TABLE OF CONTENTS

EXECUTIVE SUMMARY

This is the fourth in a series of quarterly reports describing the activities performed under Contract No. DE-AC21-94MC31160. Our analyses of Hot Gas Stream Cleanup (HGCU) ashes and descriptions of filter performance address aspects of filter operation that are apparently linked to the characteristics of the collected ash or the performance of the ceramic barrier filter elements. Task 1 is designed to generate a data base of the key characteristics of ashes collected from operating advanced particle filters (APFs) and to relate these ash properties to the operation and performance of these filters. Task 2 concerns testing and failure analysis of ceramic filter elements.

Under Task 1 during the past quarter, we analyzed a sample of ash from the gasification facility located at DOE/METC. We also performed additional analyses on gasifier ashes from tests carried out by M.W. Kellogg, Texaco, and KRW between 1988 and 1991. These additional analyses were intended to strengthen and clarify correlations that we have observed between specific surface area, uncompacted bulk porosity, specific gas flow resistance, drag-equivalent diameter, and tensile strength. Task 2 efforts during the past quarter focused on mechanical and thermal testing of new Refractron and Schumacher candle filter material.

Plans for the next quarter include analyses of ashes that we hope to obtain from General Electric's gasification facility in Schenectady, NY. We also plan to complete the design of a high-temperature test device intended to measure the uncompacted bulk porosity of aggregates of ash formed at temperatures commonly encountered in operating APFs. We will be evaluating software that will be used to construct the interactive data base of HGCU ash characteristics. Specimens of recently received Schumacher filters are being machined in preparation for nondestructive density and ultrasonic velocity measurements. Following the completion of these measurements, mechanical and thermal testing of the new Schumacher material will commence.

INTRODUCTION

This is the fourth quarterly report describing the activities performed under Contract No. DE-AC21-94MC31160. Task 1 of this contract concerns analyses of HGCU ashes and descriptions of filter performance that are designed to address the problems with filter operation linked to the characteristics of the collected ash. Task 2 of this contract includes characterization of new and used filter elements. Some of the problems observed at the Tidd and Karhula PFBC facilities include excessive filtering pressure drop, the formation of large, tenacious ash deposits within the filter vessel, and bent or broken candle filter elements. These problems have been attributed to ash characteristics, durability of the ceramic filter elements, and specific limitations of the filter design. In addition to these problems related to the characteristics of PFBC ashes, our laboratory characterizations of gasifier and carbonizer ashes have shown that these ashes also have characteristics that might negatively affect filtration. Problems with the durability of the filter elements are being addressed by the development and evaluation of elements constructed from alternative ceramic materials.

To identify which ash characteristics can lead to problems with filtration, we have assembled 235 ash samples from eleven facilities involved in METC's HGCU program. We have analyzed many of these ashes with a variety of laboratory tests. Physical attributes of the particles that we have examined include size distribution, specific surface area, particle morphology, and bulk ash cohesivity and permeability. We have also performed a range of chemical analyses on these ashes, as well as characterizations of agglomerates of ash removed from filter vessels at Tidd and Karhula. We are in the process of assembling the data obtained in these studies into an interactive data base which will help the manufacturers and operators of high-temperature barrier filters tailor their designs and operations to the specific characteristics of the ashes they are collecting.

In order to understand the thermal and mechanical behavior of the various types of ceramic materials used in hot gas filtration, we have been performing hoop and axial tensile tests, thermal expansion, compression, and creep evaluations of these materials at temperatures up to 1800 °F. Nondestructive testing methods we perform on filter specimens include density and ultrasonic velocity. To date we have evaluated various characteristics of Dupont/Lanxide PRD-66, Dupont composite, 3M composite, IF and P Fibrosics, Refractron, and Schumacher materials.

OBJECTIVES

Task 1 has two primary objectives. The first is to generate a readily accessible data base of the key characteristics of ashes collected from operating advanced particle filters. The second objective is to relate these ash properties and the contents of the data base to the operation and performance of the advanced particle filters and filter components. The first objective includes formatting the data base and collecting, analyzing, and maintaining ashes from operating HGCU facilities. The second objective of this task involves the collection

of operating histories from advanced particle filters, correlating these histories with ash characteristics, interpreting these correlations, and communicating our conclusions in the various venues prescribed by the U.S. Department of Energy's Morgantown Energy Technology Center (DOE/METC).

The objective of Task 2 is to develop an overall understanding of the thermal and mechanical behavior of hot gas filter materials. This objective includes the creation of a materials property data base which will allow the prediction of the behavior of these materials in hot gas cleanup environments. Pertinent tests will be carried out on specimens of unused filter material and also on filter elements that have been exposed in actual operating environments. Nondestructive test techniques will be applied to filter elements to characterize the strength and durability of these elements without rendering them unusable. This task will also evaluate the adequacy and completeness of manufacturers' quality assurance/quality control plans for manufactured filter elements.

TASK 1 RESEARCH ACTIVITIES

During the past quarter, we analyzed a sample of ash from the gasification facility located at DOE/METC. The sample was provided by Richard Dennis of DOE/METC who requested a full analysis of this sample. We also performed additional analyses on gasifier ashes from tests carried out by M.W. Kellogg, Texaco, and KRW between 1988 and 1991. These additional analyses were intended to strengthen and clarify correlations that we have observed between specific surface area, uncompacted bulk porosity, specific gas flow resistance, drag-equivalent diameter, and tensile strength. We planned to characterize the size distribution of several of these samples; however, the device we use to perform this measurement is down for repair. We expect to have the device repaired soon. The ash samples we studied during the past quarter are described in Table 1.

Table 1
Gasifier Ash Samples from the HGCU Data Base Characterized during the Past Quarter

ID #	Source	Brief description
2800	M. W. Kellogg	Transport Reactor Test Unit (TRTU) run G4 filter fines
2803	M. W. Kellogg	TRTU run G101 filter fines
2832	M. W. Kellogg	TRTU run H-1962-G3A filter fines
2834	M. W. Kellogg	TRTU run H-1962-G5C filter fines
2838	M. W. Kellogg	TRTU run H-1962-G7A filter fines
2840	M. W. Kellogg	TRTU run H-1962-G8A filter fines
2678	Texaco M.R.L.	run L8902-04 filter vessel ash pot solids

Table 1 (continued)

ID #	Source	Brief description
2550	KRW	fluidized bed gasification char (82 % carbon)
2556	KRW	TP-037-9: C-110 outlet composite
2557	KRW	TP-037-9: C-115 gasifier outlet composite
2558	KRW	TP-037-9: C-120 outlet composite
2559	KRW	TP-037-9: SC 41 hopper composite
2560	KRW	TP-037-9: C-121 hopper (4/25/88)
2561	KRW	TP-037-9: C-121 hopper (5/1/88)
2562	KRW	TP-037-9: C-121 hopper (4/28/88)
4170	DOE/METC	pilot-scale gasifier

Ashes generated during gasification processes differ significantly from ashes from PFBC and conventional pulverized-coal (PC) fired combustion facilities. The most distinctive chemical characteristic of most gasifier ashes is their high value of loss-on-ignition (LOI) due to the high carbon content remaining in the ash. The results of our mineral analysis of the DOE/METC gasifier ash sample (ID # 4170) are presented in Table 2 along with results of mineral analyses we performed earlier on two ash samples from early gasification tests carried out at M.W. Kellogg's Transport Reactor Test Unit. Like ashes from other processes where sorbents are used for sulfur control, the addition of sorbents during the gasification process is reflected in relatively high concentrations of calcium and/or magnesium in the ash. Of the two M.W. Kellogg samples described in Table 2, ID # 2800 was generated without added limestone, and limestone was added to the process during the generation of ID # 2803.

Table 2
Chemical Analyses of M.W. Kellogg and DOE/METC Gasification Ashes, % wt.*

constituent ID #	2800	2803	4170
Li_2O	0.02	0.02	0.02
Na_2O	0.59	0.51	0.59
K_2O	1.4	1.4	0.07
MgO	0.53	1.3	10.9
CaO	1.4	18.2	33.3
Fe_2O_3	5.8	4.6	1.17
Al_2O_3	58.9	42.3	17.4
SiO_2	29.6	22.5	31.8
TiO_2	0.67	0.5	1.49
P_2O_5	0.13	0.09	0.53
SO_3	0.94	8.6	0.32
LOI	47.2	40.7	35.9
soluble $SO_4^=$	0.36	3.5	<0.2
Equilibrium pH**	8.2	11.1	10.2

* Quantities measured prior to the most recent reporting quarter are shaded.
** Equilibrium pH is dimensionless.

Physically, gasification ashes are also quite different than PC and PFBC ashes. Tables 3, 4 and 5 summarize the analyses we performed on gasifier ashes generated by M.W. Kellogg, KRW, Texaco, and DOE/METC.

Table 3
Physical Characteristics of M.W. Kellogg Gasification Ashes*

quantity ID #	2800	2803	2832	2834	2838	2840
specific surface area, m^2/g	58	32	300	241	353	69
Stokes' MMD, µm	16	16	18	16	14	15
uncompacted bulk porosity, %	89	86	84	87	88	84
drag-equivalent diameter, µm	1.58	1.65	1.34	1.51	1.30	2.14
specific gas flow resistance, in H_2O·min·ft/lb	1.7	3.4	8.9	3.4	3.6	3.2
tensile strength, N/m^2	2.7	2.0	1.3	0.8	0.4	0.5
true particle density, g/cm^3	2.44	2.40	2.14	2.29	2.27	2.31

* Quantities measured prior to the most recent reporting quarter are shaded.

Table 4
Physical Characteristics of KRW Gasification Ashes*

quantity ID #	2550	2556	2557	2558	2559	2560	2561	2562
specific surface area, m^2/g	278	112	108	184	135	218	381	293
uncompacted bulk porosity, %	94	93	93	95	92	95	95	96
drag-equivalent diameter, µm	0.14	0.99	0.93	0.28	0.95	0.26	0.26	0.25
specific gas flow resistance, in H_2O·min·ft/lb	45	1.3	1.5	6.4	2.0	7.4	7.8	4.5
tensile strength, N/m^2	3.5	0.3	0.3	2.5	0.3	3.0	1.8	1.1
true particle density, g/cm^3	2.17	2.11	2.08	2.14	2.18	2.12	2.12	2.17

* Quantities measured prior to the most recent reporting quarter are shaded.

Table 5
Physical Characteristics of Texaco and DOE/METC Gasification Ashes*

quantity ID #	2678	4170
specific surface area, m^2/g	88	140
uncompacted bulk porosity, %	92	94
drag-equivalent diameter, µm	1.16	0.08
specific gas flow resistance, in H_2O·min·ft/lb	1.1	101
tensile strength, N/m^2	0.6	0.6
true particle density, g/cm^3	2.62	2.87

* Quantities measured prior to the most recent reporting quarter are shaded.

In general, the gasification ashes we have analyzed have very high specific surface areas. Because filtering drag is accumulated as the gas being filtered passes over the surfaces of the particles in the filter cake, high specific surface areas generally correlate with small values of drag-equivalent diameter. (Drag-equivalent diameter incorporates the effects of particle morphology on filtering drag. The effect of the structure of the filter cake on drag is determined by the filter cake porosity. Therefore, filtering drag is a function of the shape of the particles in the filter cake and the porosity of the cake.)

The relationships between the specific surface area data and drag-equivalent diameters measured for the various groups of gasification ashes listed in Table 1 are presented in Figure 1. Where sufficient data are available to identify a trend, the expected correlations between high specific surface areas and small values of drag-equivalent diameters can be seen. We believe that process differences cause each group of samples to exhibit a distinct relationship between these two variables. Differences in the way the particles were generated almost certainly caused the distribution of pore sizes on the surfaces of the

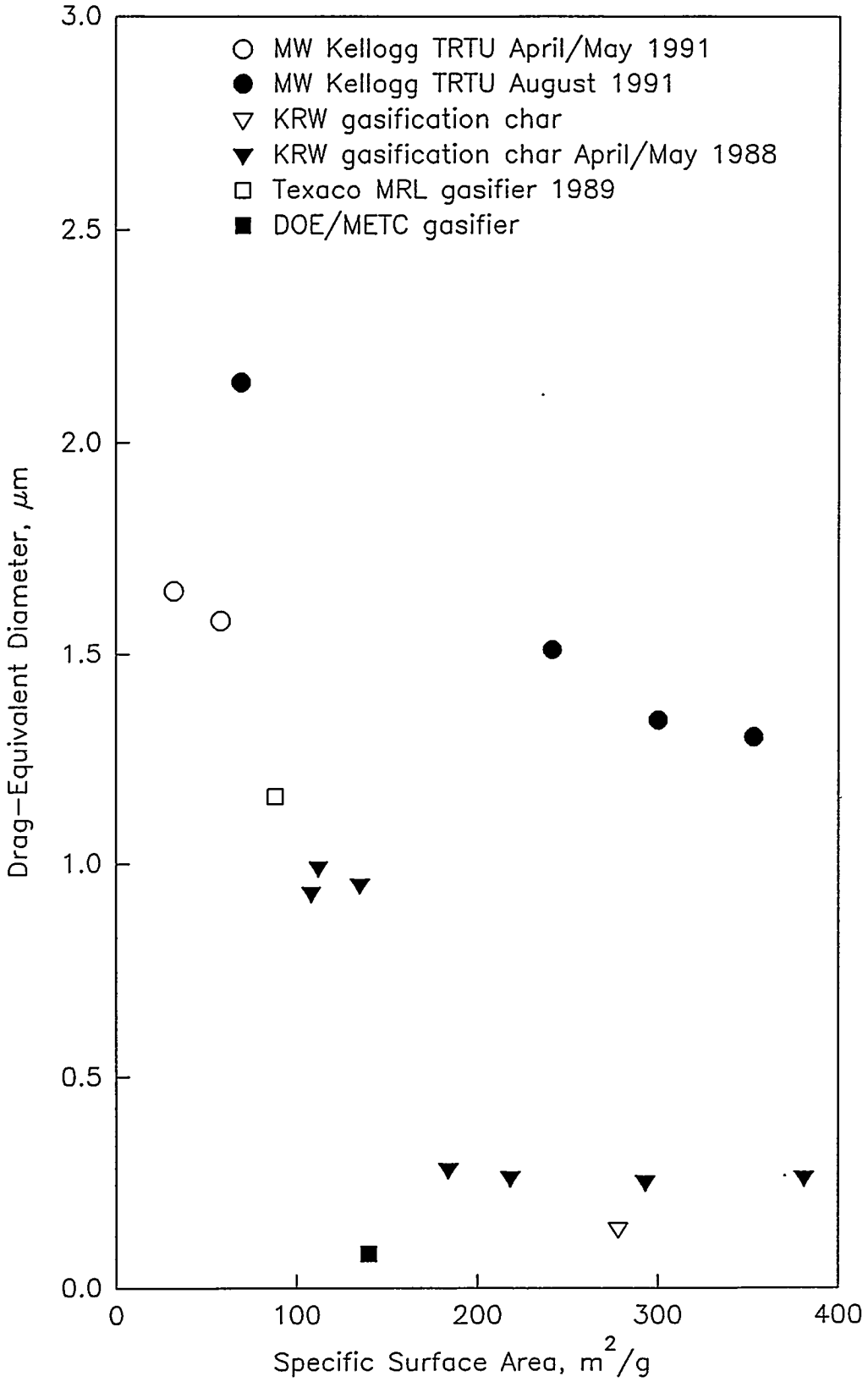

Figure 1. Relationship between specific surface area and drag-equivalent diameter for gasification ashes in the HGCU data base.

particles to differ. Similarly, the proportion of the total surface area that is contained within the ash particles would be expected to differ according to the gasification process used. These two differences in the nature of the total surface area of the various ash samples affects the correlation between specific surface area and drag-equivalent diameter. First, the BET method for measuring surface area includes any surface area found in the interior of the particles. The vast majority of gas being passed through the simulated filter cake during the determination of drag-equivalent diameter (and flue gas passing through actual filter cakes) flows over the surfaces of the particles and not through them. Therefore the internal surface area measured by the BET method has little, if any, effect on filtering drag. In a similar manner, the BET method includes the surface area contained in very fine pores on the surfaces of the particles. However, gas flowing over the surfaces of the particles does not enter pores whose sizes are on the order of the mean free path of the gas molecules. This effect also causes the BET measurement to be more sensitive to surface area than the permeability method we use to measure the drag-equivalent diameter.

Of all the gasification ashes listed in Table 1, the two ashes exhibiting the lowest permeabilities to gas flow (or the highest specific gas flow resistances) were ID # 2550 and ID # 4170. Even though these ashes would be expected to form filter cakes with porosities on the order of 94 % (the uncompacted bulk porosity value measured for each of these ashes), the morphologies of the particles in these two samples are the ultimate cause of their high resistance to filtering flow. Although other ashes listed in Table 1 have higher values of specific surface area than these two ashes, ID # 2550 and ID # 4170 exhibited the lowest values of drag equivalent diameter of all the gasification ashes we tested.

When these two ashes were examined with a scanning electron microscope (Figures 2 and 3), the fineness of their particle size distributions was readily apparent. Figure 2 demonstrates that, on a number basis, ID # 2550 is composed predominantly of ultrafine particles having diameters less than 0.5 μm. The sample also contains a much smaller number of particles with diameters around 5 to 10 μm. (On a mass basis, these larger particles almost certainly dominate the size distribution of the ash, however, we have not yet been able to measure the size distribution of this ash because of the malfunction of our sedigraph.) In Figure 3 it is apparent that the size distribution of ID # 4170 is much like that of ID # 2550, except that ID # 4170 contains very few particles larger than 5 μm diameter, and no particles with diameters larger than 10 μm.

The size distribution of ID # 4170 was measured in a recent evaluation of a laser-based device to be used at the Power Systems Development Facility. The measured data, which are shown in Figure 4, show a distinctly bimodal distribution with a volumetric median diameter of 1.8 μm. Because of the appearance of the particles in ID # 4170 in the SEM photographs shown in Figure 3, we are skeptical that the distribution shown in Figure 4 accurately represents the actual size distribution of this sample. We believe that the process used to prepare and deagglomerate the sample prior to its characterization by laser-based light scattering failed to fully separate the primary particles. In this process, a

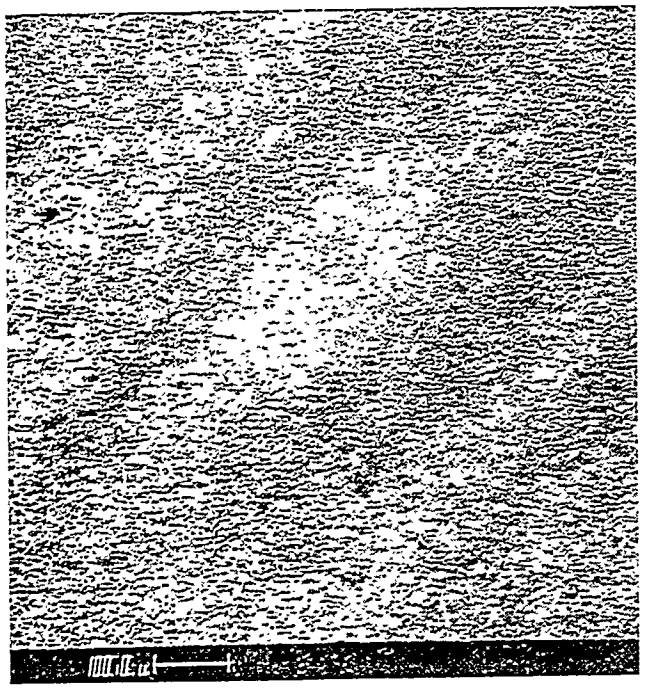

a

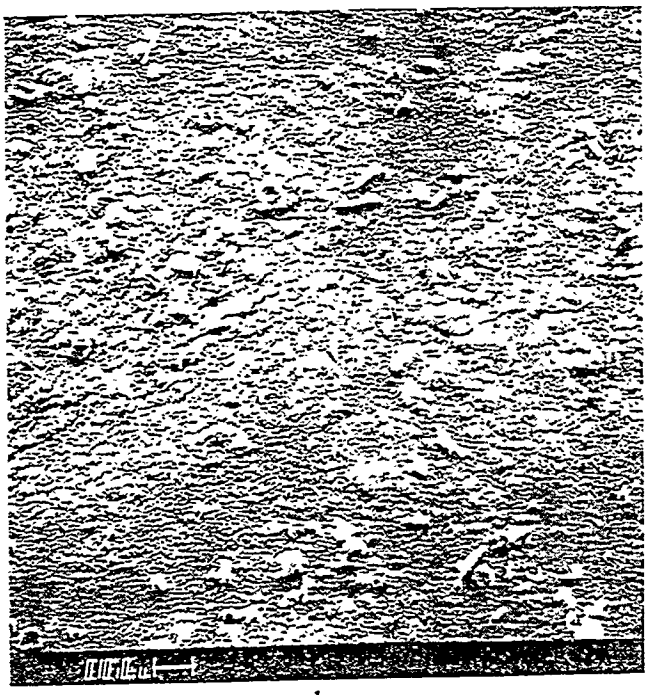

b

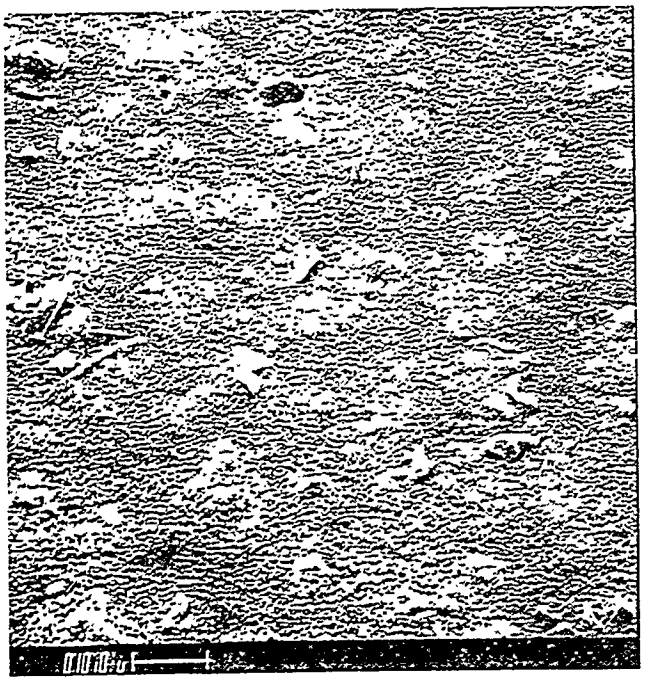

c

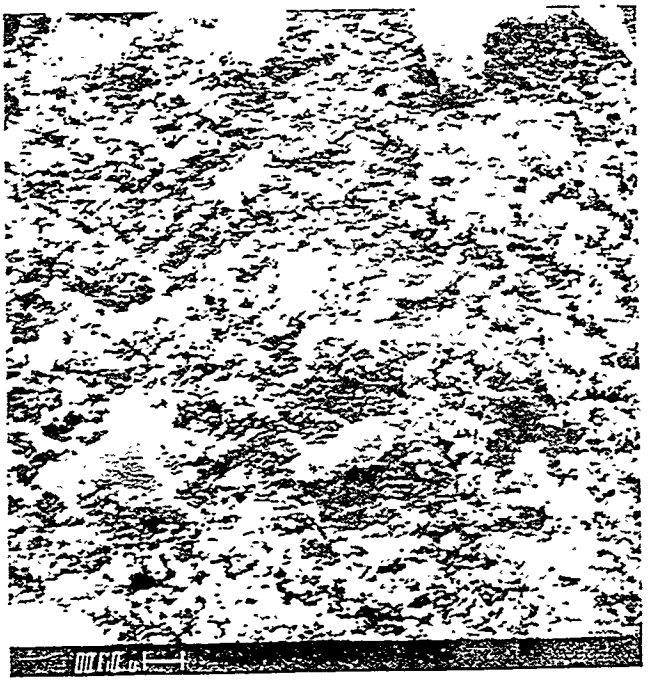

d

Figure 2. Representative SEM photographs of gasifier char (ID # 2550) taken at a) 100X, b) 500X, c) 1000X, and d) 5000X.

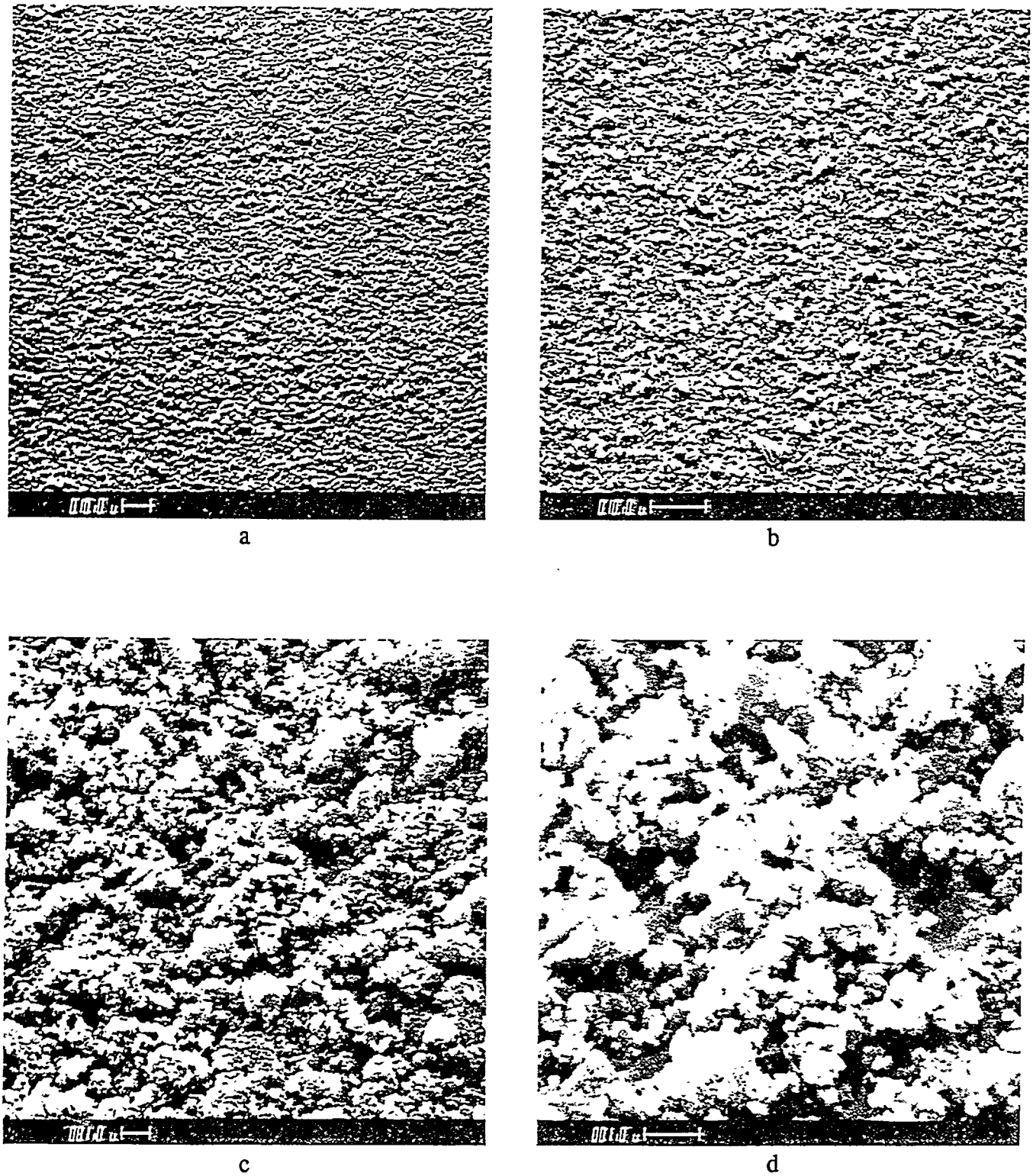

Figure 3. Representative SEM photographs of gasifier ash (ID # 4170) taken at a) 500X, b) 1000X, c) 5000X, and d) 10000X.

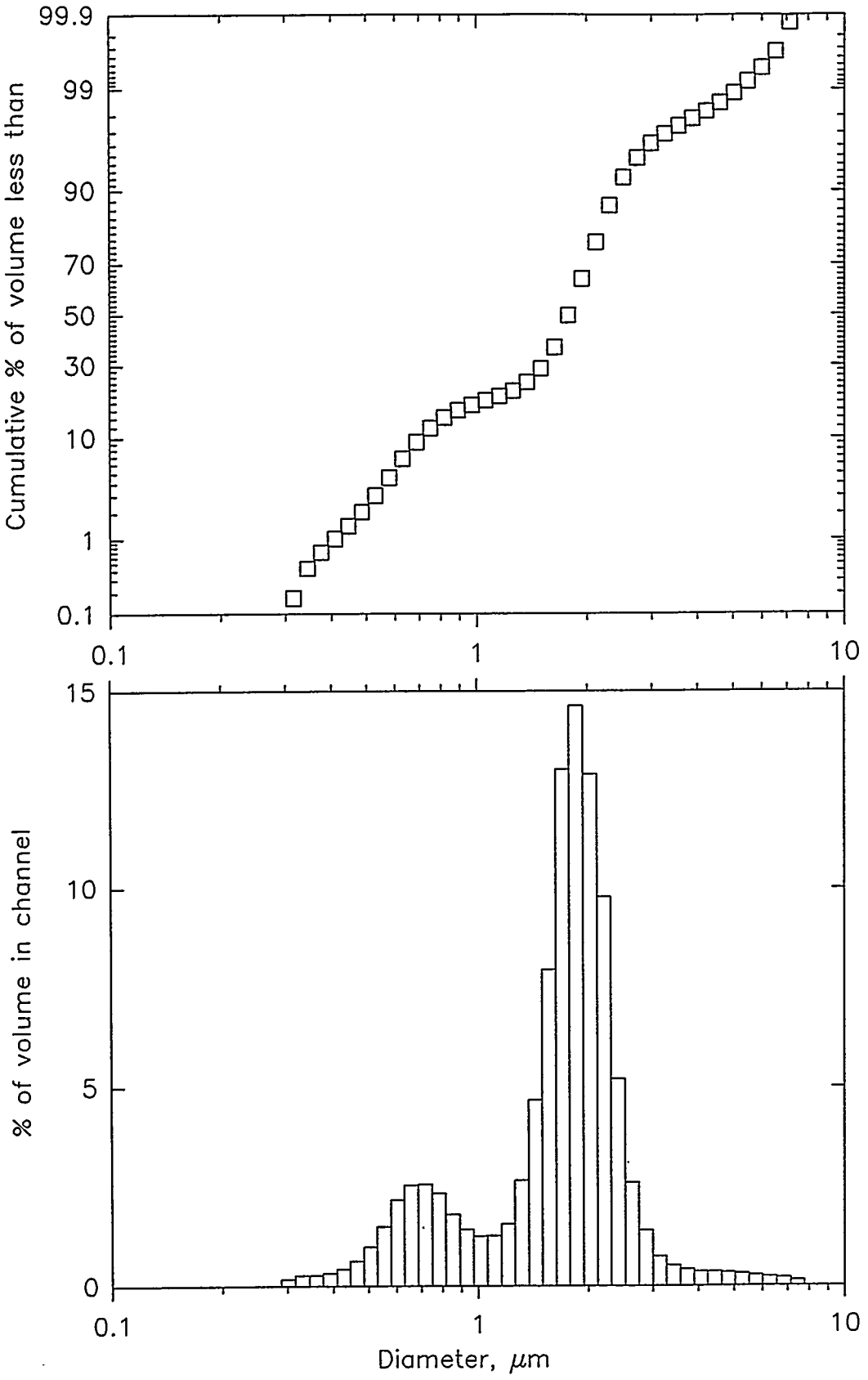

Figure 4. Cumulative and differential size distributions of ash from the DOE/METC gasifier (ID # 4170) measured by a laser-based particle size analysis system and presented on the basis of assumed particle volume.

portion of the sample was suspended in a mixture of water and two types of surfactants and the suspension was then agitated with an ultrasonic probe. This type of process is often used to successfully deagglomerate fine particles, however, it has also been known to cause primary particles to agglomerate. Based on our SEM observations of this sample and our experiences with ultrasonic agitation of dilute suspensions, we believe that the larger peak in the bimodal distribution shown in Figure 4 results from agglomerates of smaller primary particles. If this larger peak is discounted, the remaining size distribution has a volumetric median diameter around 0.7 μm instead of the 1.8 μm volumetric median diameter if the larger peak is included. In either case, the sample is composed of very fine particles, and 1.8 μm serves as an upper bound of the volumetric median size of the particles.

Another factor which may lower the median diameter even lower than the 0.7 μm value discussed above is the absence of any particles smaller than 0.29 μm in the measured distribution even though the device is supposedly able to identify and account for particles as small as 0.12 μm. Once again, based on the SEM photographs in Figure 3, the sample does appear to contain a significant proportion of primary particles smaller than 0.29 μm. These experiences during the measurement of the size distribution of ID # 4170 highlight some of the difficulties that are often encountered with samples containing a large proportion of ultrafine particles. (As with ID # 2550, we plan to quantify the size distribution of ID # 4170 with our sedigraph when it is repaired.)

Overall, these observations indicate that gasification ashes can exhibit extremely low permeabilities which can be traced to the presence of a high proportion of ultrafine particles. Consequently, it may be difficult to maintain a reasonable pressure drop in the filtration of these gasification ashes.

In general, the gasification ashes we tested exhibit very high uncompacted bulk porosities, which indicates that they are highly cohesive. (High uncompacted bulk porosities are generally associated with ashes having fine size distributions and/or irregular particle shapes. Gasification and PFBC ashes often have both of these characteristics.) However, these gasification ashes also generally exhibit relatively low tensile strengths. Normally, we would expect that highly cohesive ashes would also have high tensile strengths. We are not yet certain what causes this anomaly with gasification ashes. The low tensile strengths we have measured for gasification ash samples may indicate that ash dislodged from filter elements during pulse cleaning cycles may break up into very small agglomerates. If this type of breakup occurs, reentrainment of previously collected ash may pose a significant problem.

TASK 2 RESEARCH ACTIVITIES

Mechanical and thermal testing of the new Refractron and Schumacher candle filter material is continuing. The test matrix used to evaluate the material is as follows:

Table 6
Test Matrix for Refractron and Schumacher Filter Materials

Test Type	Orientation	RT	1600 °F	1700 °F	1800 °F
Tensile	Hoop	6			
	Axial	4	4	4	4
Tensile Creep	Axial		4	4	
Thermal Expansion	Hoop	2----------			
	Axial	2----------			
Microstructure					

Hoop and axial tensile results for the new Refractron material are given in Table 7. The average axial strength at room temperature was 1150 psi; the average hoop strength was 2130 psi. A plot of tensile strength versus temperature is given in Figure 5. Creep evaluations are in progress and no creep was detected after about 150 hours at 1550 °F. Testing will continue by increasing temperature and/or stress levels. Axial thermal expansion is summarized in Table 8 and Figure 6.

Table 7
Tensile Data for New Refractron Candle Material

Candle	Specimen #	Temp., °F	Ultimate strength, psi	Modulus, Msi	Strain-to-failure, in./in.	Remarks
4-471	TN-AX-12	70	1152	5.88	0.000196	
4-471	TN-AX-17	70	1250	6.67	0.000187	
2-469	TN-AX-5	70	910	4.82	0.000189	
2-469	TN-AX-11	70	1272	5.06	0.000251	
4-471	TN-AX-18	1600	1394	1.82	0.001300	
4-471	TN-AX-13	1600	1746	1.68	0.001400	
2-469	TN-AX-7	1600	1600	3.48	0.002250	
4-471	TN-AX-21	1600	1520	2.72	0.001640	
2-469	TN-AX-2	1700	768	1.79	--	1
4-471	TN-AX-20	1700	796	2.77	0.000690	
2-469	TN-AX-6	1700	948	2.45	0.000975	
4-471	TN-AX-19	1700	1214	4.30	0.000925	
2-469	TN-AX-10	1800	976	2.24	0.000600	
4-471	TN-AX-14	1800	989	3.33	0.000400	
2-469	TN-Hoop-1	70	2000	--	--	2
2-469	TN-Hoop-2	70	2100	--	--	2
2-469	TN-Hoop-3	70	1980	--	--	2
4-471	TN-Hoop-4	70	2190	--	--	2
4-471	TN-Hoop-5	70	2470	--	--	2
4-471	TN-Hoop-6	70	2040	--	--	2

1 Flags slipped during test
2 Load-time only

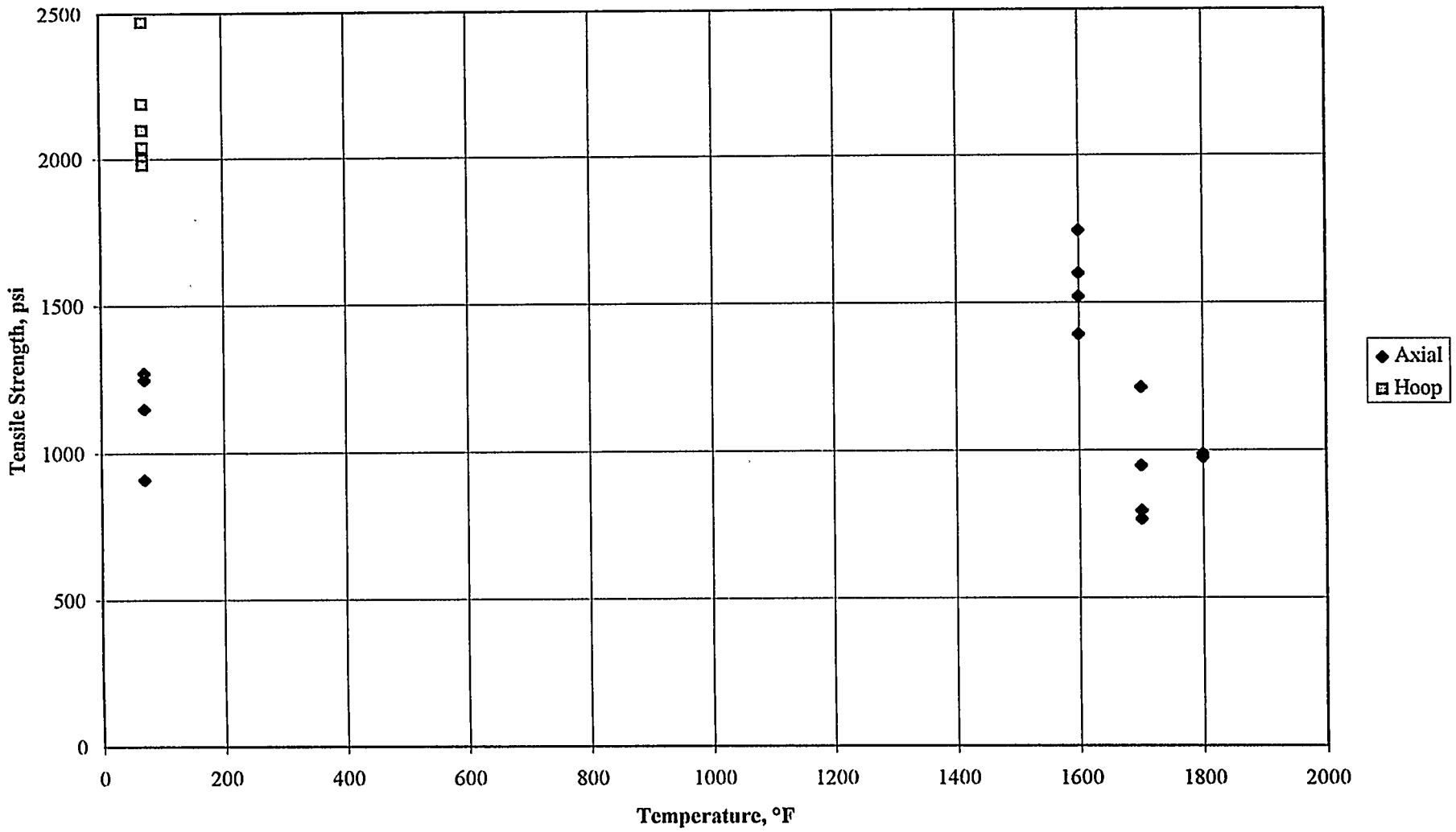

Figure 5. Tensile strength vs. temperature for new Refractron material.

Table 8
Axial Thermal Expansion for New Refractron Candle Material

Filter #	Temperature, °F	Unit Thermal Expansion, mils/inch
2-469	78	0.00
	102	0.03
	206	0.22
	315	0.51
	401	0.88
	500	1.28
	602	1.55
	700	1.74
	801	2.01
	915	2.33
	1000	2.58
	1104	2.90
	1205	3.20
	1301	3.50
	1402	3.80
	1501	4.04
	1602	4.30
	1700	4.58
	1801	4.84
	1901	5.13
	2002	5.43
	78	0.09
4-471	77	0.00
	101	0.04
	202	0.23
	301	0.47
	402	0.86
	500	1.22
	602	1.48
	700	1.71
	806	1.96
	905	2.23
	1001	2.54
	1102	2.87
	1207	3.16
	1307	3.47
	1402	3.78
	1503	4.01
	1601	4.24
	1702	4.54
	1811	4.84
	1907	5.08
	2001	5.38
	76	0.09

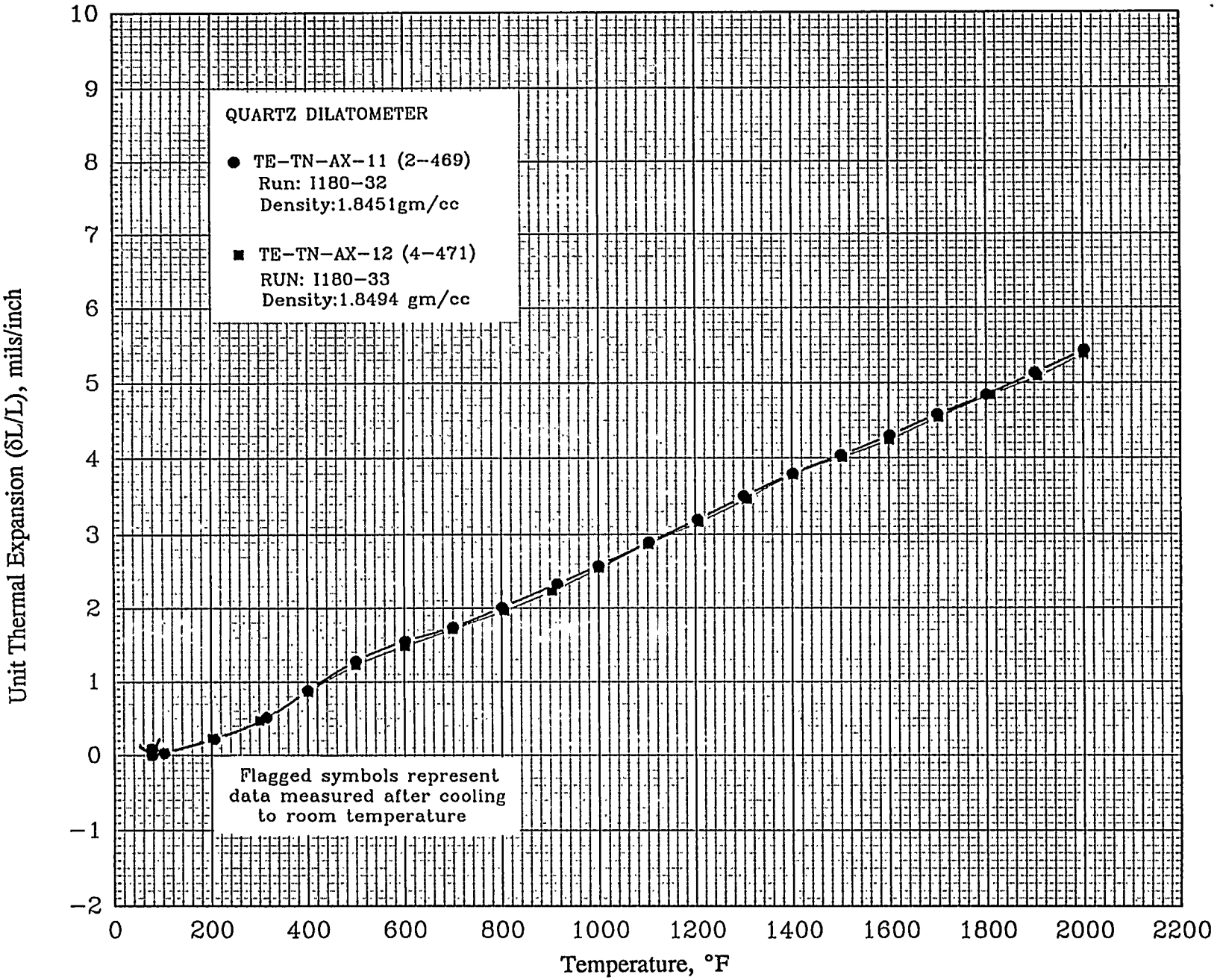

Figure 6. Axial thermal expansion of new Refractron candle filter.

New Schumacher filters were received and specimens are currently being machined according to the cutting plans given in Figures 7 and 8. When machining is complete, nondestructive density and ultrasonic velocity measurements will be made and then mechanical and thermal tests will commence.

FUTURE WORK

Plans for the next quarter include completion of the design of the uncompacted bulk porosity test device described in our second quarterly report, evaluation and selection of software for the presentation of the HGCU data base, and characterization of samples that we expect to receive from the General Electric gasification facility in Schenectady, NY. Nondestructive density and ultrasonic velocity measurements will be made on the Schumacher filters that were recently received. Mechanical and thermal tests will follow these measurements. Tests of the new Refractron material will continue.

TE-Hoop, Tn-Hoop specimens to be as-received ID and OD x 1.000" thick

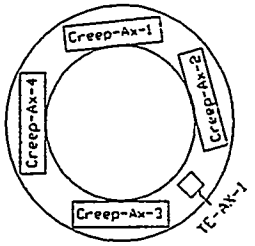

Cutting Plan for Section 1

All creep specimens to be 7.000" x 0.9995" x 0.250"
TE-AX specimen to be 3.000" x 0.375" x 0.375"

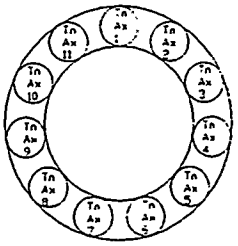

Cutting Plan for Section 2

All tensile specimens to be 0.400" dia. x 4.10"
Specimen head may have small flat due to insufficient wall thickness

Figure 7. Cutting plan for Schumacher candle 344E-295.

TE-Hoop, Tn-Hoop specimens to be as-received ID and OD x 1.000" thick

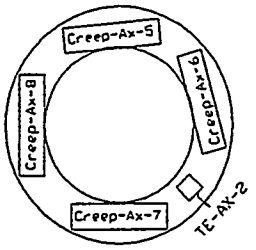

Cutting Plan for Section 1

All creep specimens to be 7.000" x 0.9995" x 0.250"
TE-AX specimen to be 3.000" x 0.375" x 0.375"

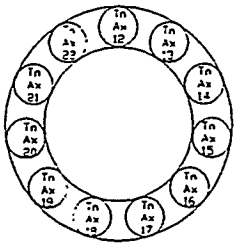

Cutting Plan for Section 2

All tensile specimens to be 0.400" dia. x 4.10"

Specimen head may have small flat due to insufficient wall thickness

Figure 8. Cutting plan for Schumacher candle 344E-309.